American Mineralogist, Volume 68, pages 1022–1028, 1983

Gainesite, sodium zirconium beryllophosphate: a new mineral and its crystal structure

PAUL B. MOORE, TAKAHARU ARAKI, IAN M. STEELE, GEORGE H. SWIHART

Department of the Geophysical Sciences
The University of Chicago, Chicago, Illinois 60637

AND ANTHONY R. KAMPF

Los Angeles County Museum of Natural History
Mineralogy-Geology Section, 900 Exposition Boulevard
Los Angeles, California 90007

Abstract

Gainesite, hypothetical end-member $Na_2Zr_2[Be(PO_4)_4]$, $a = 6.567(3)$, $c = 17.119(5)$Å, $Z = 2$, tetragonal, space group $I4_1/amd$, is a new species from the Nevel (Twin Tunnels) pegmatite, Newry, Oxford County, Maine. Crystals occur as up to 1 mm simple tetragonal bipyramids with $p\{111\}$ dominant. The color is delicate pale bluish lavender, hardness = 4 on Mohs' scale, luster vitreous, conchoidal fracture, specific gravity 2.94. It is uniaxial (+), $\omega = 1.618(2)$, $\varepsilon = 1.630(2)$. The mineral occurs in small crevices in cleavelandite associated with monoclinic roscherite and minor eosphorite. It is named in honor of Richard V. Gaines.

$R = 0.055$ for 1072 independent reflections. Eight atoms occur in the asymmetric unit of structure and five of these are disordered. Be, P, and O(3) are half-occupied while Na(1) and Na(2) are each approximately one-eighth occupied. The structure is based on an open framework of composition $[^{[6]}Zr_2{}^{[4]}Be{}^{[4]}P_4O_{16}]^{2-}$. The $[BeP_4O_{16}]^{10-}$ pentameric cluster is reminiscent of the zunyite, $[Si_5O_{16}]^{12-}$ anionic fraction.

Bond distance averages are $^{[6]}Na(1)$–O = 2.49, $^{[12]}Na(2)$–O = 3.32, $^{[6]}Zr$–O = 2.062, $^{[4]}Be$–O = 1.621 and $^{[4]}P$–O = 1.512Å. Smaller alkalies (Li^+, Na^+) appear to partition in Na(1) and larger alkalies (Na^+, K^+, Rb^+, Cs^+) appear to partition in Na(2).

Introduction

In June, 1947, the late Mr. Neal Yedlin of New Haven, Connecticut, collected a tiny (5 mm × 5 mm × 5 mm) specimen of an unknown mineral from the Nevel (Twin Tunnels) Quarry on Plumbago Mountain, Newry, Oxford County, Maine. No further specimens were found until quite recently. Dr. Carl Francis of the Harvard Mineralogical Museum located two hand specimens in the museum's collection. One of these, generously provided by Dr. Francis, proved to be the same kind of material. The type specimen (U.S. National Museum 114848 TYPE), a micromount, constituted the basis of this study. Since limited material did not allow detailed wet chemical analysis and since elements of atomic number less than fluorine could not be detected on the electron microprobe, we elected to determine the crystal structure and utilize it as a chemical analytical tool as well.

The mineral *yedlinite* is a recently described hydrated oxychloride of lead and chromium from the Mammoth Mine, Tiger, Arizona and like our present mineral was first found by Mr. N. Yedlin (McLean *et al.*, 1974). Unfortunately the name "yedlinite" applied to the Newry mineral has crept into the popular literature, since New England micromounters were aware of the unusual properties of this mineral but were unaware of the pre-emption of the name for the Arizona mineral.

The mineral gainesite is named in honor of Dr. Richard V. Gaines of Pottstown, Pennsylvania. Long a fancier and collector of minerals, his professional interests have brought him around the globe appraising sources of beryllium in pegmatites. In addition, he has published numerous professional papers on mineral chemistry and mineral associations. Over the years, he has attempted to maintain a complete collection of beryllium mineral species and it is only fitting that a beryllium mineral be named after him.

The species and name were approved by the International Commission on New Minerals and New Mineral Names (IMA). The type specimen has been deposited in the U.S. National Museum (USNM 114848 TYPE).

0003–004X/83/0910–1022$02.00

Description and properties

Physical properties

Gainesite is rather unique in its appearance, although only the three specimens known to exist were inspected. It occurs as lustrous well-formed, clear, interlocking, tetragonal bipyramidal crystals of simple habit up to 0.5 mm in greatest dimension. The mineral occurs in small crevices associated with monoclinic roscherite and minor eosphorite within interlocking plates of albite var. *cleavelandite*. The color is delicate pale bluish-lavender, hardness = 4 on Mohs' scale and the luster is vitreous. The fracture is conchoidal and cleavages were not observed. Small sections and shards are nearly colorless in transmitted light. The mineral is practically insoluble in 1:1 HCl solution at room temperature. The specific gravity as determined by the sink-float method in methylene iodide–toluene solution is 2.94(2). Under the electron microprobe beam or ultraviolet light it does not fluoresce. It is uniaxial (+) birefringence moderate, ω = 1.618(2), ε = 1.630(2), in blue-filtered white light. The forms are $p\{111\}$ dominant with occasional small $c\{001\}$. The only common accessory pegmatite mineral with which it could possibly be confused is zircon which possesses similar morphology. Indeed, the unusual color for gainesite is what prompted further investigation.

Crystallographic properties

Since the crystal structure analysis occupies most of the discussion in this contribution, only the descriptive mineralogic information will be presented here. Gainesite is tetragonal holosymmetric, $I4_1/amd$, a = 6.567(3), c = 17.119(5)Å, as determined by least-squares refinement using data from a Picker FACS-1 automated diffractometer with Mo$K\alpha$ radiation. One of the advantages resulting from a three-dimensional crystal structure analysis is that a calculated powder pattern can be obtained. This is given in Table 6.

Chemical composition

Despite the relatively simple structure of gainesite, its chemistry is quite complex. Since the mineral is a pegmatite hydrothermal product, a large number of diverse cations could play some role in its chemistry. The total water content was not determined due to the meager quantity of available material. Four major elements and twelve minor elements were detected.

Initially, several grains were studied in an ARL electron microprobe. The qualitative concentrations of major elements indicated a simple formula, but with complex substitutions at the minor element level. Operating conditions included 15 kV, 800 nA beam current and 10 sec counts at each spot. Standards included zircon (Zr), synthetic zinc oxide (Zn), apatite (P), pollucite (Cs), diopside glass (Mg, Si), synthetic anorthite (Al), microcline (K), hortonolite (Mn, Fe) and anorthite-70 glass (Na). Wavelength dispersive analysis (ADP crystal) was used for zirconium, zinc, phosphorus, rubidium and cesium. The remaining elements were analyzed using energy dispersive analyses. Hafnium, tantalum and niobium were sought and found to be undetectable. Total oxides indicated a deficit of another element or elements, with atomic number less than 11(Na).

Therefore, a grain was submitted for study on a modified AEI IM-20 ion microprobe, as sufficient material was not available for more conventional analyses, especially for Li, Be, and B. Of the three elements, B was not detected but Li and Be were present in substantial amounts. The results are included in Table 1. The relatively high errors do not admit a precise determination of amounts present and we therefore used data from the refined crystal structure to assess the roles of these cations. The counts for Li were ratioed to those from a feldspar standard which had 4 ppm Li with no matrix corrections. The Be analysis was based on relative ion yields among elements.

Three separate grains were studied by electron microprobe and a fourth grain from the same sample was also extracted for the ion microprobe analysis. Based on Z = 2 or assumed anion charge of 32^- for ideal $Na_2Zr_2[Be(PO_4)_4]$ and Table 1, the following formula is suggested:

Table 1. Gainesite: chemical analyses

	1	1a	2	3	4
Cs_2O	1.93	1.82 - 2.03	0.085	-	-
Rb_2O	0.11	±0.02	0.007	-	-
K_2O	1.45	1.30 - 1.64	0.192	-	-
Na_2O	6.81	5.94 - 7.30	1.367	10.04	2
Li_2O	1.7	±1.1	0.708	-	-
ZnO	4.11	±0.14	0.314	-	-
FeO	0.54	0.45 - 0.62	0.047	-	-
MnO	0.83	0.54 - 1.00	0.073	-	-
SrO	0.15	±0.01	0.009	-	-
CaO	0.86	0.80 - 0.90	0.095	-	-
MgO	0.30	0.22 - 0.40	0.046	-	-
BeO	2.8	±1.4	0.696	4.05	1
Al_2O_3	1.21	1.16 - 1.22	0.148	-	-
ZrO_2	33.0	32.2 - 33.4	1.667	39.92	2
SiO_2	0.59	±0.01	0.061	-	-
P_2O_5	45.0	44.9 - 45.3	3.945	45.99	4
Total	101.4		9.46	100.00	9

[1,1a]Electron probe analysis on three small grains for Cs, K, Na, Fe, Mn, Ca, Mg, Al, Zr and P. The range of values is given in 1a. Electron probe analysis on a fourth grain for Rb, Zn, Sr and Si. Their errors are listed in 1a. Three to six analysis points were taken on each grain. Concentrations <0.1 weight percent include Ba, Hf, Ta, Nb, Cr, Ti and F. Li and Be were determined from a fifth grain on an AEM-IM-20 ion microprobe. B was shown to be <5 ppm.

[2]Cation formula unit content balanced against 32 electrons.

[3]Calculated weight percent oxides for $Na_2[Zr_2Be(PO_4)_4]$.

[4]Cation content for $Na_2[Zr_2Be(PO_4)_4]$, the formula unit.

		Total	Charge
$Na(1)_1$	$:Na_{0.76}Mn^{2+}_{0.07}Fe^{2+}_{0.05}Li^{1+}_{0.12}$	1.00	+1.12
$Na(2)_1$	$:Cs_{0.09}Rb_{0.01}K_{0.19}Na_{0.61}Sr_{0.01}Ca_{0.09}$	1.00	+1.10
Zr_2	$:Zr_{1.67}Zn_{0.31}Mg_{0.05}$	2.03	+7.40
Be_1	$:Be_{0.70}Li_{0.15}Al_{0.15}$	1.00	+2.00
P_4	$:P_{3.95}Si_{0.05}$	4.00	+19.95
	Sum	9.03	+31.57

Remainder: $Li_{0.43}$

The cations in Table 1 were grouped according to increasing effective ionic radii, using the tables of Shannon and Prewitt (1969). Octahedrally coordinated zirconium, zinc and magnesium closely match and were grouped together. A slight excess occurs at this site and probably reflects analytical error or some ion partitioning elsewhere. The minor silicon appears to associate with phosphorus. The largest cations were placed in the large channel site Na(2). Sodium evidently predominates in both sites Na(1) and Na(2). Since heavier cations also occur at Na(2), this is the reason why a scattering curve for K^+ was employed at this site.

The problem remains with lithium. The ion microprobe analysis of lithium has a large uncertainty, and the difficulty is augmented by the multifarious roles the lithium ion can play in a crystal structure. Minor Li^+ was added to the Be and Na(1) sites to provide complete occupancy at these sites. Remaining in Table 1 is $Li_{0.43}$ in the formula unit. This could represent error in the analysis or additional occupancy in the disordered channel of the structure. In fact, computing the density from this formula including total lithium and the refined cell parameters, the result is 2.84 g cm^{-3}, lower than the observed specific gravity of 2.94. We have no explanation for this discrepancy.

Accepting the major component at each site, the complex formula above can be reduced to a rather simple "end-member" formula, that is: $Na_2Zr_2[Be(PO_4)_4]$, Z = 2. Evidently no such composition has been recorded and it is not known if this formula is a true end-member formula.

Table 5 clearly shows that the two alkali sites are quite different in size, with $^{[6]}Na(1)$–O = 2.49Å and $^{[12]}Na(2)$–O = 3.32Å. Since distances greater than 4.00Å were not calculated, the latter coordination sphere is not known. But clearly $r_{Na(2)} \gg r_{Na(1)}$. This considerable difference in Table 5 suggests that the two sites behave quite differently. The symbol Na was used for these sites because it is believed to be the predominant cation in both of them. Na(1) should have a refined occupancy parameter slightly less than 1/8 (due to minor Li) and Na(2) should have a number greater than 1/8 (due to Cs). It must be noted that the scattering curve for K^+ was used for Na(2) since Na^+ gave unreasonably large occupancy in the early stages of structure refinement.

Experimental details

The gainesite crystal selected for the structure analysis was from the type specimen at the U.S. National Museum (Smithsonian Institution). Numerous precession and Weissenberg photographs and one Gandolfi-mount powder pattern clearly established the unique nature of the species and established uniquely the space group $I4_1/amd$. The crystal selected for structure study was a small clear pyramid, about 0.3 mm in diameter. The simple crystal development and near-equant cross-section allowed a rather precise measurement of the positions of the vertices, and definition of five faces. Absorption correction by the Gaussian integral method (Burnham, 1966) with low total linear absorption coefficient, μ = 2.03 cm^{-1} (Mo$K\alpha$), resulted in the small absorption correction as expected. Initially, we suspected that the composition was $Na_2Zr(PO_4)_2$, Z = 4; subsequently, a computation of the absorption coefficient for the far more complex cell contents showed that μ = 2.16 cm^{-1} (Mo$K\alpha$) so no recalculation was considered necessary.

Intensities were collected on a Picker FACS-1 automated diffractometer with graphite-monochromatized Mo$K\alpha$ radiation. Background counting time on each side of a peak was 20 sec, scan speed 2° min^{-1}, scan width 4.0° to 4.8°. Data collection was limited to $\sin\theta/\lambda < 0.80$.

Symmetry equivalent reflections were found to be equal within standard error after absorption correction, and averaged to provide 1072 independent reflections for the data set.

Solution and refinement of the structure

Patterson synthesis clearly demonstrated the $\{\bar{4}2m\}$ point symmetry for Zr, which was sufficient to phase the majority of intensities. Successive Fourier syntheses led to a definition of the major structural features. Some atomic positions were only partly occupied, suggesting that a complementary relationship exists between the alkalies and the anionic radicals. Refinement and difference Fourier synthesis resulted in the resolution of two alkali, one phosphorus, one zirconium and three independent oxygen atoms. At R = 0.14, a difference synthesis revealed the Be atom. Incidentally, this was one example when the structure analysis was used as a chemical analytical tool since at this stage no ion microprobe analysis had been undertaken for the very light elements. A calculation of bond distances and inspection of the electron density profile suggested a new set of scattering curves: Na^+ for Na(1), K^+ for Na(2), Zr^{4+} for Zr, Be^{2+} and Al^{3+} for Be, P^{5+} for P and O^{1-} for O. Since no contradictions earlier appeared for space group $I4_1/amd$, three atomic sites—Be, P and O(3)—must be only half-occupied, each for steric reasons. Therefore, half-occupancies were fixed for these site populations. Any ordered model of full populations and vacancies would either force the appearance of superstructure reflections or a subgroup of the space group. Scattering curves for these ionic states were obtained from Cromer and Mann (1968). In a final refinement, anomalous dispersion corrections from Cromer and Liberman (1970) were applied

to all cations. Full-matrix anisotropic least-squares refinement for 1072 $|F_o|$ and 41 variable parameters (1 scale factor, 11 atomic coordinate parameters, 3 site occupancy parameters, 26 anisotropic thermal vibration parameters; independent data; variable parameter ratio = 26.1:1) converged to

$$R = \frac{||F_o| - |F_c||}{\Sigma F_o} = 0.055.$$

The final cycle minimized $\Sigma_w||F_o|-|F_c||^2$ where $w = \sigma^{-2}(F)$.

Atomic coordinate parameters are given in Table 2, thermal vibration parameters in Table 3, anisotropic thermal vibration ellipsoids in Table 4, bond distances and angles in Table 5, observed and calculated powder diffraction data in Table 6. The structure factors are in Table 7.[1]

Description of the structure

In gainesite, eight unique atomic positions occur in an asymmetric unit of the crystal structure. Three of these—Be, P, and O(3)—are only half-occupied as noted before and the two independent alkali positions, Na(1) and Na(2), are on the average only one-eighth occupied each. We shall see that the second phenomenon also results from steric effects. In fact, it may be more instructive to write the formula for the minimum equipoint rank number in $I4_1/amd$, that is Z = 4: $NaZr[Be_{0.5}(PO_4)_2]$. To best display the structure, we note that a composition of the elements of the space group *Imma* with the elements 4_1 and 4_3 gives the desired tetragonal space group, *viz.*:

$$\{Imma\} \cdot \{4_1, 4_3\} = \{I4_1/amd\}$$
$$\text{Order} \quad 16 \qquad 2 \qquad 32$$

Since *Pmma* is contained in *Imma* and since *Pmma* is a two-sided plane group, the strategy is then to utilize only those equipoints common to both *Pmma* and $I4_1/amd$ to draw the structure. Such a diagram appears in Figure 1 and loci of some of the 4_1-screws were placed to facilitate picturing the whole structure.

The structure type, evidently new to scientific intelligence, is based on a $[Zr_2Be(PO_4)_4]$ framework. The ZrO_6 octahedron is fully occupied, the P- and Be-tetrahedral

[1] To obtain a copy of Table 7, order Document AM-83-226 from the Business Office, Mineralogical Society of America, 2000 Florida Avenue, N.W., Washington, D.C. 20009. Please remit $1.00 in advance for the microfiche.

Table 2. Gainesite: atomic coordinates

Atom	S	E	M	x	y	z
Na(1)	m	16	0.135(6)[1]	0	0.0352(33)	0.0213(7)
Na(2)	m	16	0.104(4)[1]	0	0.6654(29)	0.0398(7)
Zr	$\bar{4}2m$	4	1.000	0	1/4	3/8
Be	$\bar{4}2m$	4	0.500[2]	0	3/4	1/8
P	m	16	0.500	0	0.1760(2)	0.1742(1)
O(1)	mm	8	1.000	0	1/4	0.2551(2)
O(2)	m	16	1.000	0	0.5645(3)	0.3781(1)
O(3)	m	16	0.500	0	0.5540(7)	0.1826(3)

[1]Na(1) had a scattering curve for Na^+, Na(2) for K^+. Note that the sum of site populations suggests quarter-occupancy. Point symmetry (S), rank number (E) and refined occupancy (M) are listed.

[2]Refined to 0.41(1) Be^{2+} + 0.09 Al^{3+}.

Table 3. Gainesite: anisotropic thermal vibration parameters†

Atom	β_{11}	β_{22}	β_{33}	β_{12}	β_{13}	β_{23}
Na(1)	198(34)	344(66)	21(5)	0	0	67(17)
Na(2)	144(21)	585(78)	27(4)	0	0	58(13)
Zr	36(1)	36	7(0)	0	0	0
Be	154(58)	154	19(6)	0	0	0
P	35(2)	53(2)	7(0)	0	0	-2(1)
O(1)	107(7)	107	10(1)	0	0	0
O(2)	109(4)	37(3)	12(1)	0	0	-3(1)
O(3)	125(10)	57(7)	16(1)	0	0	2(3)

†Coefficients in the expression $\exp-[\beta_{11}h^2 + \beta_{22}k^2 + \beta_{33}\ell^2 + 2\beta_{12}hk + 2\beta_{13}h\ell + 2\beta_{23}k\ell]$. Estimated standard errors refer to the last digit except for those coefficients related by symmetry. The parameters are $\times 10^4$.

Table 4. Gainesite: parameters for the ellipsoids of vibration†

Atom	i	u_i	θ_{ia}	θ_{ib}	θ_{ic}	$B_{eq}(Å^2)$
Na(1)	1	0.096(31)	90	120(4)	30(4)	3.93(48)
	2	0.208(18)	180	90	90	
	3	0.311(29)	90	30(4)	60(4)	
Na(2)	1	0.170(14)	90	108(3)	18(3)	5.24(50)
	2	0.178(13)	180	90	90	
	3	0.372(24)	90	18(3)	72(3)	
Zr	1	0.088(1)	····not determined·····			0.69(1)
	2	0.088	····not determined·····			
	3	0.102(1)	90	90	0	
Be	1	0.169(25)	90	90	0	2.52(38)
	2	0.183(34)	····not determined·····			
	3	0.183	····not determined·····			
P	1	0.088(2)	0	90	90	0.80(2)
	2	0.101(2)	90	129(9)	141(9)	
	3	0.112(2)	90	141(9)	51(9)	
O(1)	1	0.124(5)	90	90	0	1.64(4)
	2	0.153(5)	····not determined·····			
	3	0.153	····not determined·····			
O(2)	1	0.089(4)	90	9(4)	81(4)	1.29(3)
	2	0.132(3)	90	81(4)	171(4)	
	3	0.154(3)	0	90	90	
O(3)	1	0.111(7)	90	173(7)	83(7)	1.68(7)
	2	0.156(7)	90	97(7)	173(7)	
	3	0.165(7)	0	90	90	

†i = ith principal axis, u_i = rms amplitude, θ_{ia}, θ_{ib}, θ_{ic} = angles (deg.) between the ith principal axis and the cell axes a_1, a_2 and c. The equivalent isotropic thermal parameter, B_{eq}, is also listed. Estimated standard errors in parentheses refer to the last digit.

Table 5. Gainesite: bond distances and angles†

Zr				**Na(1)**		
2 Zr-O(1)	2.053(3)			2 Na(1)-O(3)$^{(4)}$	2.41(2)	
4 -O(2)	2.066(2)			2 -O(3)$^{(1)}$	2.44(1)	
average	2.062 Å			2 -O(2)$^{(1)}$	2.61(2)	
				average	2.49	
4 O(1)-O(2)$^{(8)}$	2.875(3)	88.54(6)°	additional:			
4 O(2)-O(2)$^{(8)}$	2.923(3)	90.04(0)		1 Na(1)-P	2.78(1)	
4 O(1)-O(2)	2.949(3)	91.46(6)		1 Na(1)-O(3)$^{(3)}$	2.82(1)	
average	2.916					
2 O(2)-Zr-O(2)$^{(3)}$		177.09(11)		**Na(2)**		
1 O(1)-Zr-O(1)$^{(8)}$		180.00		1 Na(2)-O(3)	2.55(1)	
				1 -O(3)$^{(3)}$	3.06(2)	
				2 -O(2)$^{(4)}$	3.17(1)	
Be				2 -O(2)$^{(1)}$	3.35(2)	
				2 -O(1)$^{(5)}$	3.42(2)	
4 Be-O(3)	1.621(5)			2 -O(3)$^{(1)}$	3.53(2)	
				2 -O(2)$^{(7)}$	3.63(2)	
2 O(3)-O(3)$^{(3)}$	2.575(9)	105.1(3)		average	3.32	
4 O(3)-O(3)$^{(4)}$	2.683(8)	111.7(2)	additional:			
average	2.647	109.5		2 Na(2)-O(2)$^{(6)}$	3.99(2)	next larger
				2 Na(2)-O(3)$^{(4)}$	1.48(1)	rejected (steric)
P						
P-O(1)	1.467(3)			1 Na(1)-Na(1)$^{(10)}$	0.86(3)	
P-O(3)$^{(3)}$	1.517(5)			1 -Na(1)$^{(3)}$	2.82(4)	
2 P-O(2)$^{(1)}$	1.531(2)					
average	1.512			1 Na(2)-Na(2)$^{(3)}$	1.11(4)	
				1 -Na(2)$^{(11)}$	2.56(4)	
O(1)-O(3)$^{(3)}$	2.351(5)	103.9(2)		2 -Na(2)$^{(4)}$	3.02(3)	
O(2)$^{(1)}$-O(2)$^{(2)}$	2.436(4)	105.4(2)				
2 O(1)-O(1)$^{(1)}$	2.492(3)	112.5(1)		1 Na(1)-Na(2)$^{(12)}$	1.35(2)	
2 O(2)$^{(1)}$-O(3)$^{(3)}$	2.518(4)	111.4(1)		1 -Na(2)$^{(3)}$	1.35(3)	
average	2.468	109.5		1 -Na(2)$^{(11)}$	2.23(2)	
				1 -Na(2)	2.45(3)	

†Estimated standard errors in parentheses refer to the last digit. The equivalent positions (referred to Table 2) are designated as superscripts and are (1) = ¾ -y, ¼ +x, ¾ +z; (2) = ¼ +y, ¼ -x, ¾ +z; (3) = x, ½ -y, z; (4) = ¾ -y, ¾ -x, ¼ -z; (5) = ¼ +y, ¾ -x, ¼ -z; (6) = ½ -x, ½ -y, ½ -z; (7) = ½ -x, y, ½ -z; (8) = ¼ -y, ¼ -x, ¾ -z; (9) = ¾ +y, ¼ +x, ¾ -z; (10) = -x, -y, -z; (11) = x, -y, -z; (12) = -x, ½ +y, -z.

centers exactly half-occupied (Table 2), leading to local domains of $[P_4BeO_{16}]$ pentameric clusters alternating with large open pockets if P–P shared tetrahedral faces are to be avoided. In fact, such a corner-sharing pentameric cluster occurs in the crystal structure of zunyite (Kamb, 1960) as $[Si_5O_{16}]^{12-}$ radicals.

The entire structure can be visualized as a $_\infty{}^3[Zr_2Be(TrO_4)_4]$ framework, where Tr symbolizes a trigonal bipyramid which arises by the fusion of two tetrahedral faces or two $(PO_4)^{3-}$ anionic radicals which are forced to share faces in $I4_1/amd$ if that site is fully occupied. In fact, a fully ordered framework formula can be conceived, having cell composition $[M_4Tr_8T_4O_{40}]$ where M and T are octahedral and tetrahedral populations respectively. The vacancies in gainesite force the composition $[Zr_4P_8(Be_2\square_2)(O_{32}\square_8)]$, where $\square$ denotes vacancy. Could such a hypothetical compound exist which would be fully ordered? Writing it as MTr_2TO_{10}, a possibility may be $^{[6]}Zr^{4+[5]}Mo_2{}^{6+[4]}Si^{4+}O_{10}$. Here all cations have inert gas configurations and such coordination numbers for those cations in oxysalt environments are known. Since charge, ionic radii and coordination number put important constraints on admissible compositions, this must be considered a hypothetical possibility.

Table 6. Gainesite: observed and calculated powder patterns†

I(obs)	d(obs)	I(calc)	d(calc)	hkℓ	I(obs)	d(obs)	I(calc)	d(calc)	hkℓ
100	6.068	100	6.131	101			2	1.596	219
30	4.240	29	4.280	004	10	1.581	4	1.586	411
20	4.065	4	4.082	112			1	1.573	228
90	3.265	60	3.284	200	10	1.530	1	1.534	413
50	3.023	36	3.036	105			2	1.533	404
40	2.881	21	2.895	211	10	1.517	4	1.523	332
20	2.597	10	2.605	204			2	1.514	1.0.11
		5	2.431	116	10	1.462	2	1.468	420
10	2.316	4	2.322	220			2	1.461	327
10	2.277	4	2.292	107	10	1.437	1	1.444	415
10	2.221	3	2.229	215	10	1.432	3	1.436	309
30	2.165	10	2.171	301			1	1.389	424
		2	2.140	008	10	1.356	4	1.360	336
		2	2.044	303	20	1.318	7	1.321	3.1.10
		1	2.041	224			2	1.316	329
30	2.012	9	2.018	312	10	1.305	3	1.310	431
		1	1.879	217			2	1.303	408
20	1.836	9	1.844	305	10	1.277	2	1.280	433
20	1.822	6	1.827	109			2	1.274	512
20	1.802	8	1.811	321			2	1.268	3.0.11
		3	1.793	208			1	1.226	435
10	1.725	1	1.735	323			3	1.211	428
30	1.673	9	1.679	316	10	1.181	1	1.183	3.2.11
20	1.637	6	1.642	400			1	1.183	1.1.14
		2	1.631	307			1	1.174	516
		2	1.608	325	20	1.145	4	1.148	3.3.10
20	1.601	5	1.606	1.1.10					

†FeK_α radiation, 114.6 mm camera diameter, Gandolfi mount. Although the film was corrected for shrinkage, the data were not corrected for absorption. Calculated data obtained from the crystal structure.

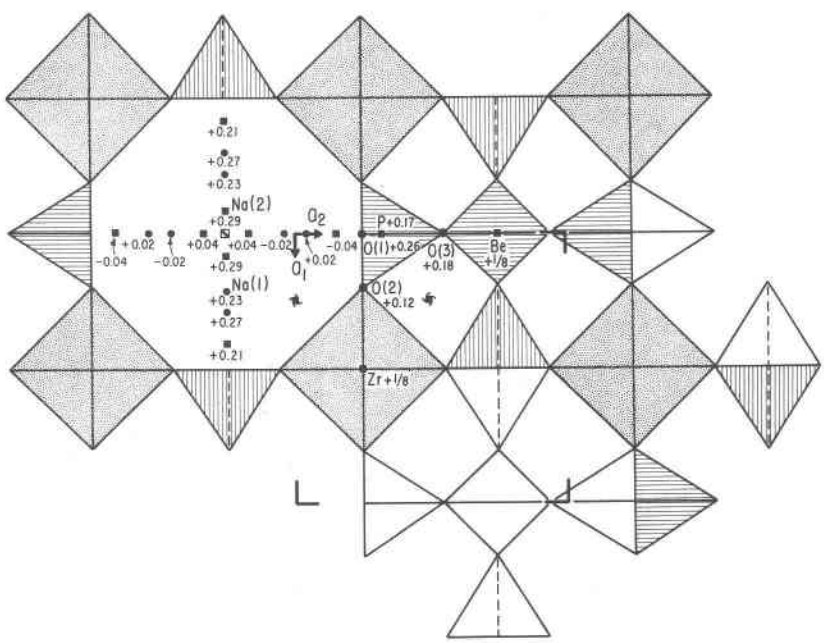

Fig. 1. Polyhedral representation of the gainesite crystal structure down [001]. The unit cell and some 4-fold screws are sketched in. The ZrO_6 octahedra are stippled. The central $[Be(PO_4)_4]$ tetrahedral pentamer is shown with ruled lines, and as edge lines only when tetrahedral faces are shared. In one region, it is omitted completely and the Na(1) and Na(2) distributions are shown instead along with $\bar{4}$ center. Heights are given as fractional coordinates in z.

For such an elegantly simple structure, gainesite is a veritable garbage basket. With the pertinent tables at hand, it is now possible to integrate its crystal chemistry. Table 5, which outlines the bond distances and angles, demonstrates that the $^{[6]}Zr$–O = 2.062Å average is about the anticipated value for major $^{[6]}Zr^{4+}$ participating in bonds to two-coordinate oxide anions. The same holds for $^{[4]}Be$–O = 1.621Å and $^{[4]}P$–O = 1.512Å. It is possible that higher oxidation of the first transition series ions may account for the lavender color of the crystal, as, for example, high-spin Mn^{3+} which has a pronounced Jahn–Teller distortion. Another unusual site involves Be, which refined to 0.82 Be^{2+} + 0.18 Al^{3+}. We note that the chemical analysis allowed (0.70 Be^{2+} + 0.15 Li^{+}) + 0.15 Al^{3+} and, in absence of further evidence, we adopt this site population.

The alkali sites are most interesting. In Figure 1, the structure diagram was deliberately drawn to show an occupied [BeP_4O_{16}] site (ruled lines), a vacant site (edge lines only for the polyhedra) and the site but occupied with alkalies only. Clearly, gross steric problems exist, particularly evident in Table 5. Included are two Na(1)–Na(1), two Na(2)–Na(2), two Na(2)–O(3), and four Na(1)–Na(2) interactions, each interaction less than 3.0Å. Each alkali site has C_s symmetry, with 16 equipoints in the cell. The average residency would be ½[for BeP_4O_{16} presence] × ½[for Na(1)–Na(1)′ or Na(2)–Na(2)′ coupled interactions] × ½[for Na(1)–Na(2) interactions] = ⅛. This appears to be the site population based on refined values given in Table 2. Note that the occupancy factor of Na(1) is a little larger than 0.125, and that of Na(2) a little smaller. Table 5 lists Na–O bond distances according to increasing values. Na(2) resides toward the center of the large disordered channel while Na(1) is located more toward its periphery. Twelve Na(2)–O distances are listed, ranging from 2.55 to 3.63Å. The average Na(2)–O = 3.32Å is close to $^{[12]}Cs$–$^{[6]}O$ = 3.28Å from Shannon and Prewitt (1969). Note that Na(2)–O(3)$^{(4)}$ = 1.48Å was rejected for reasons of steric hindrance. The next larger distance is Na(2)–O(2)$^{(6)}$ = 3.99Å, which was arbitrarily cut off. This larger alkali site suggests that Cs^{+} can be accommodated in the structure type. With cations of a range in radii occupying this site, the thermal vibration parameter is more likely a mean residency parameter, the greatest anisotropy being in the [001] direction. Na(1) has six nearest neighbors which define a distorted trigonal prism. The next larger distance is to a cation and this is accepted as the cutoff for the anion coordination sphere about Na(1). The average $^{[6]}Na(1)$–O = 2.49Å is slightly larger than Na–O = 2.42Å in Shannon and Prewitt. This site, too, has a range of cation populations and, likewise, its thermal parameter is extremely anisotropic. Beryllium, too, possesses a large thermal parameter. The three sites, Na(1), Na(2) and Be, possess the largest thermal parameters (Tables 3 and 4), doubtless due to a variety of cations at each of these sites.

When a structure is known, it is desirable to calculate a powder pattern and compare it with the experimental results. This is presented in Table 6 and the agreement is satisfactory. An electrostatic valence balance calculation was performed, but owing to the great variety of cations over specific alkali sites, it is deemed unworthy of further report.

Acknowledgments

We thank Mr. Paul E. Desautels of the U.S. National Museum of Natural History (Smithsonian Institution) and Dr. Carl A. Francis of the Harvard Mineralogical Museum for loan of the specimens used in this study.

This work was supported in part by the grant NSF EAR-19483 (Geochemistry) awarded to P.B.M.

References

Britton, D. and Dunitz, J. D. (1973) A complete catalogue of polyhedra with eight or fewer vertices. Acta Crystallographica, A29, 362–371.

Burnham, C. W. (1966) Computation of absorption correction, and the significance of the end effect. American Mineralogist, 51, 159–167.

Cromer, D. T. and Liberman, D. (1970) Relativistic calculation of anomalous scattering factors for X-rays: Los Alamos Scientific Laboratory, University of California Report LA-4403, University of California-34.

Cromer, D. T. and Mann, J. B. (1968) X-ray scattering factors computed from numerical Hartree-Fock wave-functions. Acta Crystallographica, A24, 321–324.

Kamb, W. B. (1960) The crystal structure of zunyite. Acta Crystallographica, 13, 15–24.

McLean, W. J., Bideaux, R. A. and Thomssen, R. W. (1974) Yedlinite, a new mineral from the Mammoth Mine, Tiger, Arizona. American Mineralogist, 59, 1157–1159.

Shannon, R. D. and Prewitt, C. T. (1969) Effective ionic radii in oxides and fluorides. Acta Crystallographica, B25, 925–946.

Manuscript received, April 23, 1982;
accepted for publication, February 25, 1983.